Application of ANSYS-Fluent Software for Innovative Stepped Dissipation Blocks Arrangement in Ogee Spillway

Mohammed Al-Fatlawi[1, a*] and Abdulhassan Al-Shuker[1, b]

[1]College of Engineering, University of Babylon, Babil, Iraq

[a]Mohammedalfatlawi.civileng1996@gmail.com and [b]abdulhassan.alshuker@coeng.uobabylon.edu.iq

*Corresponding author

Abstract. The Ogee Spillway is one of the most crucial flood control structures, and it is developed at the same time as dams. The Ogee Spillway's downstream portions experience scouring due to flow, a problem that persists in reality. This paper aims to investigate the hydraulic performance of stepped block dissipater using a three-dimensional simulation model. The dissipated block was given a new distribution that may be one, two, or three rows in the transverse arrangement at a right angle with the path lines. The numerical simulations for flow and scour were performed using the computational fluid dynamics (CFD) ANSYS-Fluent software. Under Froude numbers ranging from 2.75 to 9.25, the sequence depth and transverse velocity distribution were measured. According to the results, the employed blocks minimized flow rates and sediment scouring throughout the stilling basin in line with suggested distributions, particularly with the Fr 4.5-9.25 range. With values in the 0.95-0.98 range of Correlation Coefficient (R^2) and 0.43-0.45 of Root Mean Square Error (RMSE) the coefficient and the comparison of the computational and experimental data looked to be in good agreement. The results proved that the stepped block configuration with (A1, A2, and A3) block distributions, where the A3 distribution appeared with good results of reducing flow velocities within the stilling basin following A1 and A2 distributions, especially with the range of Fr 4.5-8.5. Also, good stability of the hydraulic jump was observed when using A3, while this was difficult to achieve by using both A1 and A2.

Keywords: Hydraulic jump; Froude number; dissipated block; velocity distribution; sequent depth.

1. INTRODUCTION

Dam construction has been a top priority across the world because of the rising need for water supply, flood control, hydroelectric power generation, and recreation. Technology advancements in the design and analysis of dams are required for improved management of water resources since protecting water is of utmost significance [1]. Spillways are a standard feature on all dams as a safety precaution against overtop. The most typical style of spillway used to discharge water from a dam or levee reservoir into the downstream channels is an ogee spillway, which is sometimes referred to as an overflow or an S-shaped spillway [2]. A typical occurrence in open channel flow is a hydraulic jump, which is most noticeable near the toe of hydraulic structures like spillways. Dissipating the extra kinetic energy downstream of the hydraulic structures is one of the major uses of a hydraulic jump. The stilling basin is the most typical type of structure used to contain hydraulic jumps to accomplish the necessary kinetic energy dissipation [3]. As it flows downstream smoothly, water going over an ogee spillway crest always stays in contact with the spillway surface. High kinetic energy water flowing over an ogee spillway can contribute to dam failure by causing erosion at the end of the spillway [4, 5]. To provide safe flow conditions and diffuse the force of the flowing water, stilling basins of various designs are employed to prevent erosion at the spillway's downstream end. Several types of blocks and end sills are typically installed in these basins to stabilize, shorten the hydraulic jump, and increase performance [6-8]. In the late 1950s, Bradley and Peterka devised the typical stilling basin, which primarily utilizes baffle blocks to dissipate the excess kinetic energy. The use of computational modeling of spillway flows is growing in the field of hydraulic engineering. To explore the impact of position, relative size, and curvature curved (in plan) on the hydraulic jump qualities and energy dissipation, Eloubaidy [9-12] initially used a cubic stepped block. It was discovered that baffle blocks effectively dissipate surplus kinetic energy under all flow conditions.

The effects of using the direction-diverting blocks installed on an ogee spillway surface with various slopes on energy dissipation are examined by Ellayn and Sun [18]. The configurations differ in spacing between rows of blocks and the number of rows. When blocks were used, the maximum reduction in Froude Number was 36%, 89%, and 93% for spillway models with slopes 1:1, 0.85:1, and 0.75:1, respectively. An experimental hydraulic model was described by [13] to assess the effectiveness of an ogee spillway. The spillway under examination has a typical ogee profile with continuous steps cut from a tangential point to the toe of a straight section of the downstream wall. The average increase in energy dissipation was found to be around 37%, which would suggest that the size of the stilling basins downstream was significantly reduced. Wedge-shaped and baffle blocks were utilized by [2] to determine their impact on the hydraulic jump characteristics. Compared to those with smooth beds, the results reveal a decrease in the jump length and subsequent depth ratio. In contrast to wedge blocks, which demonstrated slower changes in bed profile, baffle blocks demonstrated rapid scour processes. As a result, more research into the hydraulics of the Ogee Spillway in terms of scour and energy dissipation seems appealing. This study aims to (1) Investigate the energy dissipation and sand blanket scour downstream of the stilling basin under 2.25-9.25 values of Fr using the CFD software ANSYS-Fluent Software. (2) Examine the impact of blockage distance on the hydraulic performance when there are 1, 2, and 3 rows of stepped blocks.

2. MODEL DESIGN AND DIMENSIONS

2.1 Model Similitude

The correlation between physical quantities in the model and the prototype is a critical problem that might be important in hydraulic flow, such as viscous effects, surface tension, and gravity effect. The Froude Number similarity requires that $V_r = \sqrt{L_r}$, the Reynolds Number scaling implies that $V_r = 1/L_r$, and the Weber Number similarity requires $V_r = 1/\sqrt{L_r}$, where $Lr = Lp/Lm$. The subscript r refers to the prototype-to-model quantity ratio, and the subscripts P and M refer to prototype and model parameters, respectively [9]. For example, when friction losses are low, and the flow is very turbulent, Fr modeling is frequently employed in spillways. Just the predominant mechanism is represented in each scenario. According to Chow (Tuna, [14]), the model flow must behave as a prototype for Reynolds Number greater than 2000 and Weber Number greater than 11, as gravity effects are always significant in free-surface flow and Fr modeling is used, so viscous and surface tension effects are negligible in the prototype [15]. A reduced prototype-to-model scale ratio should be employed to reduce scale effects if they are expected to be substantial in a model. The gravity effect predominates with a geometric scale ratio of 50:1 or 25:1, but the viscous effect may be abolished [16]. Physical models are built with dimensions that achieve a geometric scale of 50:1 when this restriction is satisfied, and the dimensions of the channel laboratory are used. Table 1 lists the similitude model ratios for this geometric scale.

Table 1: Physical similitude relations [9].

Parameter	Relations
Discharge	$Q_r = V_r L_r^2 = L_r^{2.5}$
Velocity	$V_r = \sqrt{L_r}$
Energy	$E_r = L_r^4$
Reynolds number	$R_r = L_r^{1.5}$
Pressure	$P_r = F_r/L_r^2$

The main spillway model is a big prototype that is scaled down to 1:100. The top portion of the primary model, as shown in Figure 1, is 10 times smaller than the spillway model. The main goal of this scenario was to gather additional information at the crest of an ogee spillway.

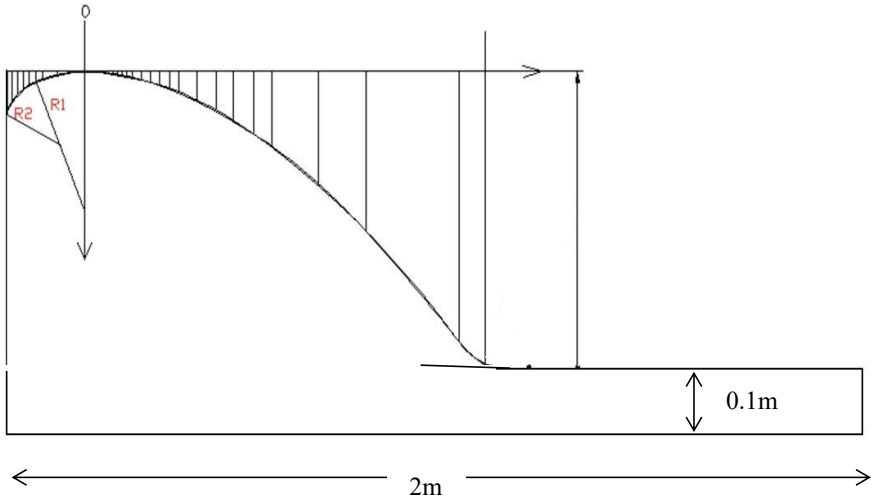

Figure 1: Schematic representation of the scale ogee spillway model.

Table 2 lists the selected case's geometric dimensions following earlier experimental findings [17], [18], [13]. The prototype width for the 1:30 model is 30×0.3=9 m, but the prototype width for the 1:3 model is 3×0.3=0.9 m, as the same flume of 0.3 m wide was utilized in the laboratory.

Table 2: Model dimensions.

Spillway length(m)	Spillway depth (m)	Crest width (m)	Spillway radius (m)	
			R1	R2
2.0	0.45	0.3	0.05	0.02

2.2 Model Set-Up

The CFD model geometry was created with the same dimensions as two cases of the two accessible

physical models using the ANSYS design model. The geometry of these two physical models (of various scales) was not constructed using the prototype dimensions they represent in the numerical modeling. The surface and body were both frozen in the geometry builder so that a fluid flow could pass through the modeling domain. Mesh creation is a crucial phase in CFD modeling that needs careful consideration. The domain had to be divided into smaller cells, where the governing equations would be solved, in order to examine the fluid flow. Fundamentally, the number of cells in the mesh determines how accurate a CFD solution is. The precision of the answer improves with increasing mesh fineness. To prevent unintended influences on the computational analysis's solution correctness and turnaround time, mesh quality was evaluated. This point becomes especially important when issues are not properly conditioned and/or complete hydrodynamic studies are considered. The examination and assessment of meshing quality are highly helpful in this situation as they help to solve the problem and type of analysis under consideration.

The measured difference between the form of the cell and the shape of an equilateral cell of similar area (for a 2D domain) or volume is known as cell skewness, according to ANSYS Inc. (for a 3D domain). Computational cells with high skewness might affect the solution's accuracy and stability. The following Equation defines equisize skewness calculation:

$$M_{eqs} = \frac{S_{eq} - S}{S_{eq}} \quad (1)$$

S and S_{eq} are the computational mesh element's area (2D) or volume (3D) and the maximum area (2D) or volume (3D) of an equilateral element whose circumscribed radius is the same as the computational mesh element's.

Cell skewness shouldn't be greater than 0.98 in the range of exquisite skewness between 0 and 1. The exquisite skewness of the computational cells (mesh) was less than 0.57 in all situations, indicating high mesh quality. The orthogonal quality is a measurement that ANSYS -FLUENT employs as another significant mesh quality indication. Directly from the discretization performed by the Fluent solver comes the orthogonal quality. The orthogonal quality scale runs from 0 to 1, and the required minimum orthogonal quality is 0.051. Orthogonal quality was attained at or above 0.70 for all numerical models, indicating extremely high mesh quality. After the model's geometry was created and meshed with the ANSYS -Fluent software, the mesh was loaded into a fluent solver. Before the simulations could begin, the solver's various parameters had to be specified. ANSYS -Fluent can solve fluid motion equations in two or three dimensions involving momentum, energy, and mass protection. When defining free surface flows in CFD models, the volume of fluid (VOF) approach is typically used. The following is the generic mass continuity equation for the fluid motion:

$$\theta_{cr,i} = \frac{0.3}{1+1.2d_{*,i}} + 0.055\left[1 - exp\left(-0.02d_{*,i}\right)\right] \quad (2)$$

Where:
d*, i is a dimensionless parameter and computed as below:

$$d_{*,i} = d_i \left[\frac{\rho_f (\rho_i - \rho_f)\|g\|}{\mu_f^2}\right]^{\frac{1}{3}} \quad (3)$$

Where ρ_i is the sediment density, ρ f is the density of the fluid; di is the diameter of sediment, μ_f is the dynamic viscosity of the liquid, $\|g\|$ is the magnitude of the gravitational acceleration. The volumetric bed-load transport rate defined by Meyer-Peter and Müller (Kuriqi et al., 2020) is:

$$\Phi_i \left[\|g\| \left(\frac{\rho_i - \rho_f}{\rho_f}\right) d_i^3\right]^{\frac{1}{2}} \quad (4)$$

Where Φ_i: is the dimensionless bed-load transport rate. Cohesionless sand that is 1.0 m thick was employed as the ground substance to calculate the degree of scouring. Moreover, the Meyer-Peter, Müller method shown in Equation (4) was used to estimate the bed-load transfer. Table 3 provides the bed-load sediment's physical characteristics.

Table 3: Physical specifications of the sediment.

Sediment Characteristics	**Values**
Species bed-load	Coarse sand
Species diameter (m)	0.005
Sediment Density (kg/m^3)	2400
Critical Shields number	0.05
The angle of response (degree)	32

2.3 Configuration and Arrangement of Standard USBR

The shape and dimensions of the block are recommended by USBR at which the upper longitudinal dimension and width of the block are selected as a function of block height [19].

2.3.1 Block Configuration

The block that was used during the study is stepped. The block that was used during the study is stepped. The height of the block was chosen to be 5 cm for all selected models. The block model was simulated with a width of 3.75 cm, and the length of the base is manufactured at 6 cm, according to Maatooq and Taleb [12], as presented in Figure 2.

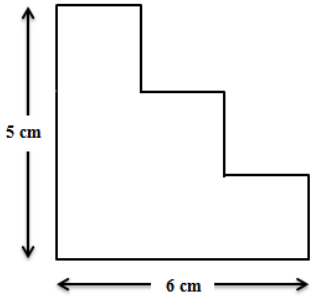

Figure 2: The configuration and dimensions of the stepped block model.

2.3.2 Block Distribution

The used blocks have been arranged at a new proposed blockage ratio "η" so they do not exceed 0.5, according to Maatooq and Taleb [12]. The calculation of the blockage ratio is according to:

$$\eta = \sum W_b / \sum (W_b + S) \quad (5)$$

Where theW_b, is the block's width, and S is the clear spacing between the adjacent blocks. Three groups of block model distributions were used; the first group is one row with two blockage ratios, the second group installed at two rows includes three different distance ratios $\bar{X}$/b, and the third group installed at three rows includes fixed distance ratios $\bar{X}$/b, where $\bar{X}$ is a distance from the front face of blocks of the first row to the front of the second row. Different blockage ratios were used when installing these blocks. The distribution of these three categories is shown in Table 4. The test was conducted to determine which method was most effective for enhancing a hydraulic jump's depth ratio and transverse velocity dispersion.

Table 4: Stepped block distribution.

Group	Configuration	No. of Rows	Blockage Ratio	Dimensions (cm)			S1 cm	S2 cm	S3 cm	S4 cm	$\bar{X}$ /b
				h	b	W_b					
A	A1	One row	37.5%(1)	5	6	3.75	5.625	3.75	-	-	-
	A2	One row	37.5%(1I)	5	6	3.75	1.875	7.5	-	-	-
	A3	One row	50%	5	6	3.75	1.875	3.75	-	-	-
B	B1	Two rows	50&37.5% (II)	5	6	3.75	1.875	3.75	5.625	3.75	1
	B2	Two rows	50&37.5% (II)	5	6	3.75	1.875	3.75	5.625	3.75	2
C	C1	Three rows	50&37.5 % (II)	5	6	3.75	1.875	3.75	5.625	3.75	3

The design approach was based on the procedure documented in Small Dam Design by USBR (1987). Different configurations have been arranged in single, double, and complex rows. The location of the first baffle block from the toe spillway was selected equal to $X_0/y_2^* = 1.3$. It was adopted as recommended by [12], where the X_0 related to the sequent depth of jump that was calculated by the Belanger equation. Since the maximum y_2^* is 17.11 cm according to the minimum incoming water level spillway, incoming Froude number X_0 was fixed at 22.24 cm downstream of the spillway for all runs undertaken. The space between the first block and the wall of the flume was equal to $0.5W_b$ for each side. Figure 3 represents a general sketch example of these used block distributions over the USBR stilling basin.

Numerical analyses are carried out for different flow conditions. For the study, unit flows Q = 0.017 m^3/sec. to 0.025 m^3/sec. was studied as an experimental study. These flow rates are the values at which the highest number of scours is observed before the baffle is placed. Solutions were conducted for 30 min. In light of the information obtained from previous studies, it is known that a period of approximately 0.5 hours is necessary for the scouring to reach a stable level. In addition, it is known that 75% and 85% of the scouring takes place

in the first half-hour and one-hour period, according to Ellayn and Sun (2012) [18]. A half-hour solution time is thought to be sufficient to provide a notion of how the scouring will start and how much it will be scoured because numerical modeling for 2D models requires a significant amount of time.

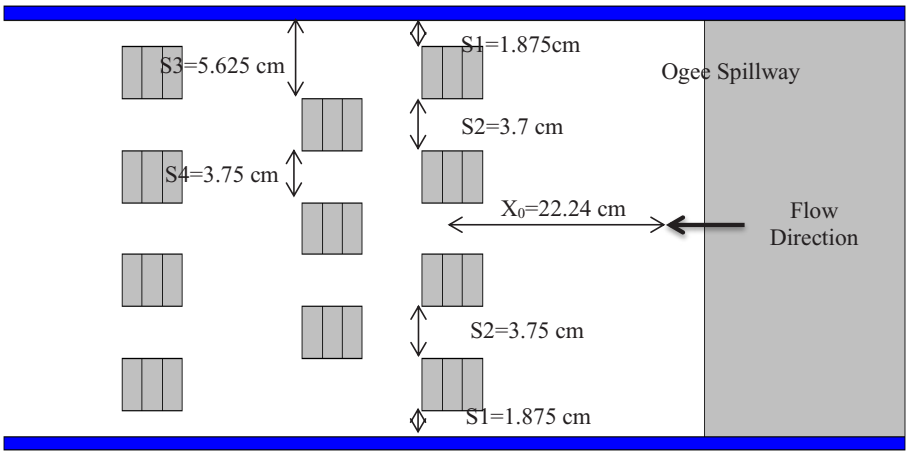

Figure 3: Stepped block distribution along the stilling basin with blocks arrangement-C1 two rows, $\bar{X}$ /b=2and η=50&37.5%II.

2.4 Scour and Stilling Basin

The stilling basin is a structure that serves as an energy absorber downstream of the spillway. The end-sill is one of the components of the stilling basin. The end-sill is important for preventing the super-critical flow from the spillway's crest from flowing into the stilling basin and hydraulic jump, which causes the flow to shift to the sub-critical flow behind the end-sill structure.

3 RESULTS AND DISCUSSION

The experiments were achieved to estimate the stepped block efficiency for improving the characteristics of a hydraulic jump, such as depth ratio, transverse velocity distribution, and scour downstream of the stilling basin.

3.1 Velocity Distribution and Sequent Depth Results

Figure 4 shows the variation of the sequent depth ratio (y_2/y_1) with the initial Froude number for all configurations A, B, and C models. This figure shows the line that represents the sequent depth ratio of a free jump of the Belanger equation. However, the configuration-B2 of group B performs better in reducing the sequent depth (y_2) than the other configurations. The observations show that this configuration has led to lengthening the roller region, consequently, increases energy dissipation. However, it grows from the length of the stilling basin.

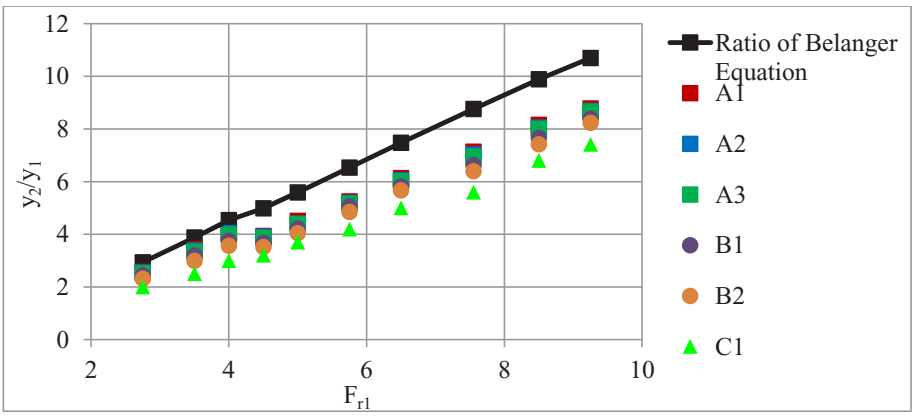

Figure 4: Sequent depth ratio for all configurations of stepped blocks.

3.2 Validation Work

To examine the precision of the outcomes of the numerical simulation performed using ANSYS-Fluent. The configuration-C1 results were contrasted with those of earlier studies by [17], [18], [12]. This comparison is illustrated in Figure 5 and demonstrates a similar pattern between the findings of the current investigation and those of the earlier studies. Nevertheless, fewer successive depth ratios are linked to employing configuration C1, suggesting that the hydraulic jump performance was enhanced using this arrangement instead of one row. In comparison to the findings of Eloubaidy (1999) [17], Ellayn and Sun (2012) [18], Maatooq, and Taleb (2018) [12], the decrease of y_2/y_1 has improved by 65%, 35%, and 20%, respectively. Correlation R2 and RMSE equal 0.95-0.97 and 0.43-0.45, respectively. Accordingly, a good convergence between the results was confirmed by previous studies [20-24]. It was possible to create a new relationship between the sequent depth ratio and the Froude number for the optimal configuration, C1;

$$\frac{y_2}{y_1} = 0.6694\mathrm{Fr}_1 + 0.354 \quad (6)$$

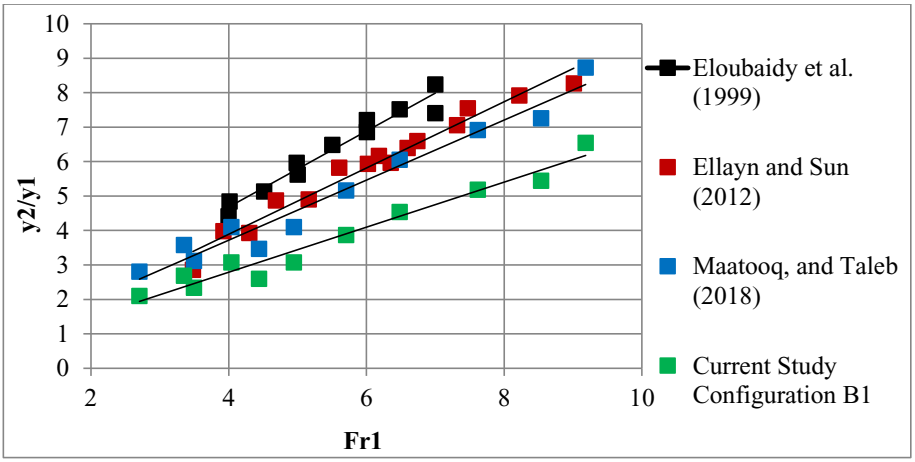

Figure 5: Comparison of the sequent depth ratio for baffle block configuration B1 with previous studies.

3.3 Scour Downstream of Stilling Basin

Figure 6 shows the unit flow rates for the $q = 89.4$ m³/hr and the scouring time that has occurred over time in the sediment downstream of the regulator. Since the energy was not dissipated by the hydraulic jump within the stilling basin, the souring depth has been exaggerated in the sand blanket. As compared to the no-stepped condition, as shown in Figure 7, the impact of stepped blocks on the downstream can be noticed. Except for the lack of a block, which is depicted by the red line in the same image, this type of block is defined by limiting the erosion that happens in the stilling basin to a ratio of up to (100%) when the Froude number is equal to (2.5). Moreover, the maximum scour value increases from 0 cm to 10 cm when the Froude number reaches a value of 9.25. According to the numerical modeling that was done, the suggested distribution C1 was differentiated in lowering sediment erosion to a distinct degree, followed by the distributions of B2, B1, A3, A2, and A1, respectively, while discussing the effects of scour in the stilling basin. The type C1 distribution of stepped blocks performed best when considering the hydraulic jump, which provides efficient energy dissipation. Even though all baffle types with a sill offer efficient defense against the scour downwind of the building.

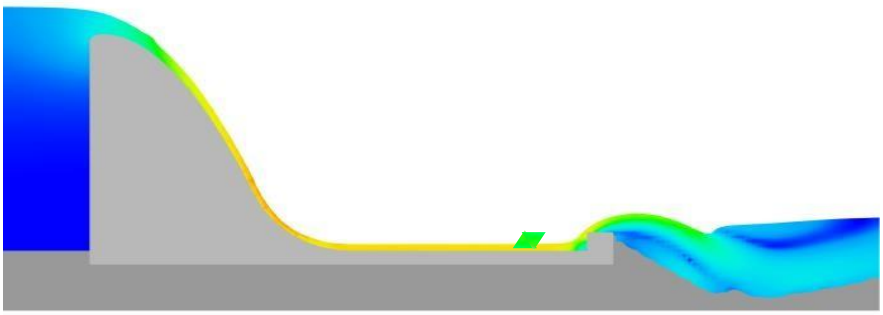

(a) No blocks under $Q = 0.025$ m³/sec, Fr1=9.25 and max. scouring = 10 cm

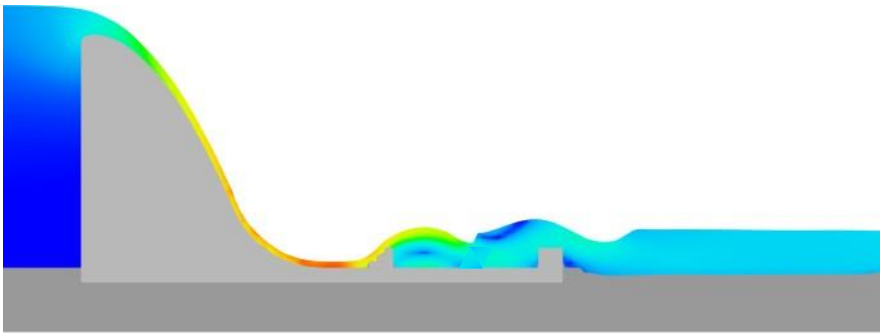

(b): Stepped blocks under Q = 0.025 m³/sec, Fr1=9.25 and max. Scouring = 0.25 cm
Figure 6: Numerical results (Without blocks and with A1) under Fr1=9.25.

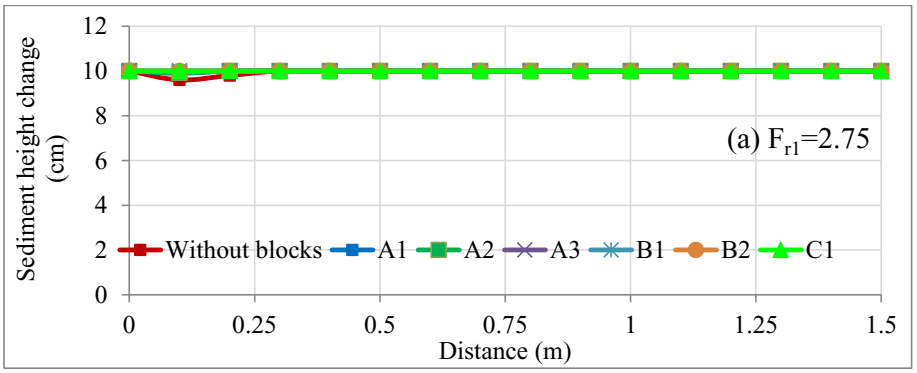

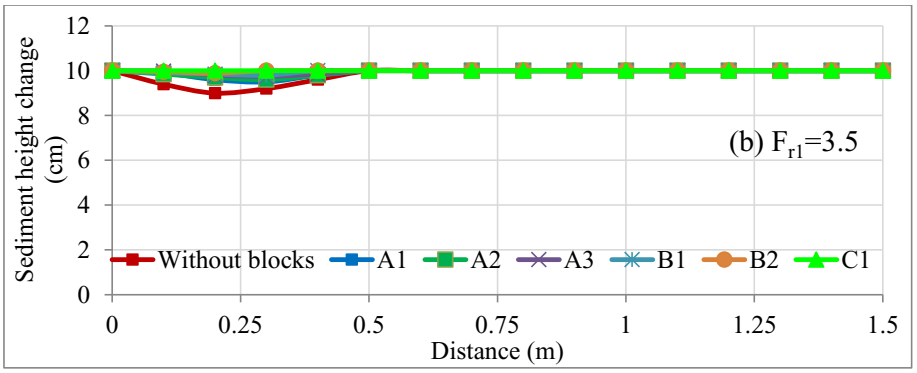

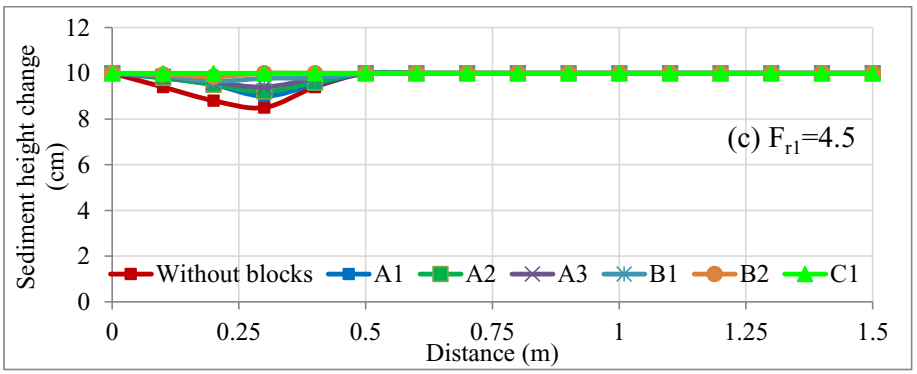

Figure 7: Scour profiles at downstream flows of the stilling basin.

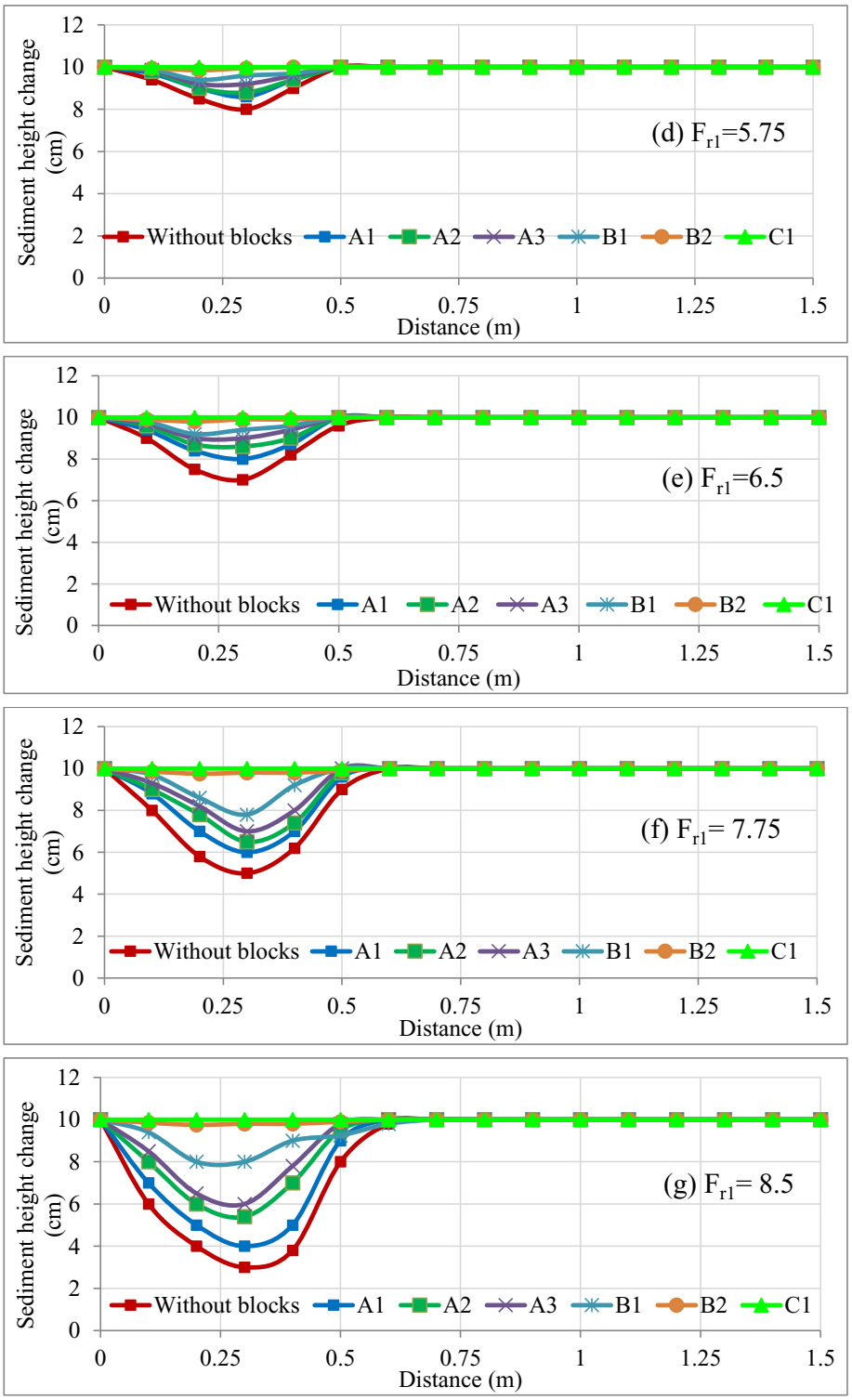

Figure 7: (continued) Scour profiles at downstream flows of the stilling basin.

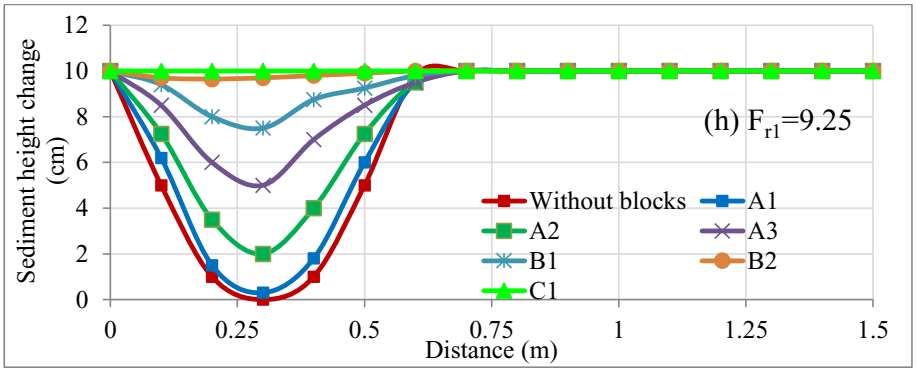

Figure 7: (continued) Scour profiles at downstream flows of the stilling basin.

4. CONCLUSIONS

The findings can be summarized as follows:

- For stepped block configuration with (A1, A2, and A3), the A3 distribution appeared with good results of reducing y_2/y_1 within the stilling basin following A1 and A2 distributions, especially with the Froude number 4.5-8.5 range. Also, good stability of the hydraulic jump was observed when using A3, which was difficult to achieve by using both A1 and A2.
- The variation of the sequent depth ratio (y_2/y_1) with the initial Fr for all stepped block distributions A, B, and C, proved that block distribution B2 was efficient in decreasing the y_2/y_1 compared to the other distributions. This decrease is a pointer to improving hydraulic performance and increasing energy dissipation along the stilling basin.
- The previous experimental works agreed with the current numerical simulation (with ANSYS -Fluent Software) results, through the values ranges 0.9585 to 0.9897 of R^2 coefficient and 0.43-0.45 of RMSE.
- According to the numerical modeling results of scour, hydraulic jump, and energy dissipation in the stilling basin, it can be said that the proposed distribution C1 was distinguished in reducing sediment erosion to a distinct degree, followed by the distribution of B2, B1, A3, A2, and A1, respectively.

REFERENCES

[1] Alwan, H. H., Kamonna, H. H., & Hashim, N. A. Evaluation of local scour development downstream an apron of different angles for an ogee spillway. Kufa Journal of Engineering. 2016; 7(3).
[2] Al-Zubaidy, R., Al-Murshidi, K. R., & Khlif, T. H. Energy dissipation by using different sizes and configurations of direction diverting blocks on spillways. Journal of Babylon University/Engineering Sciences. 2014.
[3] Muhsun, S. S., & Al-Sharify, Z. T. (2018). Experimental work and CFD model for flowrate estimating over ogee spillway under longitudinal slope effect. International Journal of Civil Engineering and Technology. 2018; 9(13): 430-439.
[4] Peltier, Y., Dewals, B., Archambeau, P., Pirotton, M., & Erpicum, S. (2018). Pressure and velocity on an ogee spillway crest operating at high head ratio: experimental measurements and validation. Journal of Hydro-environment Research. 2018; 19(1): 128-136.
[5] Daneshfaraz, R., Ghaderi, A., Akhtari, A., & Di Francesco, S. On the effect of block roughness in ogee spillways with flip buckets. Fluids. 2020;5(4): 182.
[6] Morales, V., Tokyay, T. E., & Garcia, M. Numerical modeling of ogee crest spillway and tainter gate structure of a diversion dam on Canar River, Ecuador. In International Conference on Water Resources CMWR. 2012.
[7] Saneie, M., SheikhKazemi, J., & Azhdary Moghaddam, M. Scale effects on the discharge coefficient of ogee spillway with an arc in plan and converging training walls. Civil Engineering Infrastructures Journal. 2016; 49(2): 361-374.
[8] Yildiz, A., Yarar, A., Kumcu, S. Y., & Marti, A. I. Numerical and ANFIS modeling of flow over an ogee-crested spillway. Applied Water Science. 2020; 10(4): 1-10.
[9] Asadi, M. E., Naeeni, S. T. O., & Kerachian, R. The effects of splitters on the downstream scour hole of overflow spillways: application of support vector regression. Water Supply. 2022; 22(2): 1905-1929.
[10] Mohammed, J. R., & Qasim, J. M. Comparison of one-dimensional HEC-RAS with two-dimensional ADH for flow over trapezoidal profile weirs. Caspian Journal of Applied Sciences Research. 2012; 1(6): 1-12.
[11] Elnikhely, E. A. Investigation and analysis of scour downstream of a spillway. Ain Shams Engineering Journal. 2018; 9(4): 2275-2282.
[12] Eloubaidy, A. F., Al-Baidhani, J. H., & Ghazali, A. H. Dissipation of hydraulic energy by curved baffle blocks. Pertanika Journal Science Technology. 1999; 7(1), 69-77.

[13] Maatooq, J., & Taleb, E. The effects of baffle blocks locations and blockage ratio on the sequent depth and velocity distribution of forced hydraulic jump. 2018.
[14] Saki, N., & Shafai Bejestan, M. (2022). Experimental Investigation of the Wedge-Shaped Deflector Installation Position Effects on the Flip Bucket Spillway Energy Dissipation. Journal of Hydraulics. 2022; 17(2): 87-106.
[15] Tuna, M. Effect of Offtake Channel Base Angle of Stepped Spillway On Scour Hole. Iranian Journal of Science and Technology. Transactions of Civil Engineering 36. 2012.
[16] Young, M.F. Feasibility Study of a Stepped Spillway. Proceedings, Hydraulics Division Speciality Conference, ASCE, New York. 2022.
[17] Sorensen, R.M. Stepped Spillway Hydraulic Model Investigation. Journal of Hydraulic Engineering, ASCE. 2020; 111(12): 1461-1472.
[18] Eloubaidy, A. F., Al-Baidhani, J. H., & Ghazali, A. H. Dissipation of hydraulic energy by curved baffle blocks. Pertanika Journal Science Technology. 1999; 7(1): 69-77.
[19] Ellayn, A. F., & Sun, Z. L. Hydraulic jump basins with wedge-shaped baffles. Journal of Zhejiang University SCIENCE A. 2012; 13(7): 519-525.
[20] Peterka, A. J. Hydraulic Design of Stilling Basins and Energy Dissipators. United States Department of the Interior, Bureau of Reclamation, Engineering Monograph No. 25, Denver CO, 4th revised printing. 1978.
[21] Alsultani, R., Karim, I. R., & Khassaf, S. I. Dynamic Response Analysis of Coastal Piled Bridge Pier Subjected to Current, Wave and Earthquake Actions with Different Structure Orientations. International Journal of Concrete Structures and Materials. 2023; 17(1): 1-15.
[22] Alsultani, R., & Khassaf, S. I. Nonlinear Dynamic Response Analysis of Coastal Pile Foundation Bridge Pier Subjected to Current. Wave and Earthquake Actions: As a model of civilian live. Resmilitaris. 2022; 12(2): 6133-6148.
[23] Alsultani, R., Karim, I. R., & Khassaf, S. I. Mathematical formulation using experimental study of hydrodynamic forces acting on substructures of coastal pile foundation bridges during earthquakes: As a model of human bridge protective. Resmilitaris. 2022; 12(2): 6802-6821.
[24] Alsultani, R., Karim, I. R., & Khassaf, S. I. Dynamic Response of Deepwater Pile Foundation Bridge Piers under Current-wave and Earthquake Excitation. Engineering and Technology Journal. 2022; 40(11): 1589-1604.
[25] Salahaldain, Z., Naimi, S. and Alsultani, R. Estimation and Analysis of Building Costs Using Artificial Intelligence Support Vector Machine. Mathematical Modelling of Engineering Problems. 2023; 10(2): 405-411.